Journal of Operation and Automation in Power Engineering
Vol. 6, No. 2, Dec. 2018, Pages: 147-156
http://joape.uma.ac.ir

# Field Oriented Control of Dual Mechanical Port Machine for Hybrid Electric Vehicle

*H. Afsharirad, M. B. B. Sharifian, M. Sabahi, S. H. Hosseini*

*Department of Electrical and Computer Engineering, University of Tabriz, Tabriz, Iran.*

***Abstract-*** *A dual mechanical port machine (DMPM) is used as an electrical variable transmission (EVT) in hybrid electric vehicle (HEV). In the conventional HEV, this machine is replaced to planetary gear box and two electric machines and makes this structure simpler. This paper presents field oriented control (FOC) for DMPM. For HEV application, drive efficiency and wide operation speed range are important. The control strategy, which uses maximum torque per ampere (MTPA) method at low speed and flux weakening (FW) method at high speed is proposed. The model of DMPM considering the magnetic coupling between two air gaps has been developed in MATLAB/Simulink and the proposed control strategy is applied to DMPM. The simulation results have been provided with a brief discussion at the end.*

***Keyword:*** Dual mechanical port machine, Field oriented control, Flux weakening, Hybrid electric vehicle, Maximum torque per ampere.

## NOMENCLATURE

| | |
|---|---|
| CVT | Continuous Variable Transmission |
| DMPM | Dual Mechanical Port Machine |
| EMF | Electromotive Force |
| EV | Electric Vehicle |
| EVT | Electrical Variable Transmission |
| FOC | Field Oriented Control |
| FW | Flux Weakening |
| HEV | Hybrid Electric Vehicle |
| ICE | Internal Combustion Engine |
| MTPA | Maximum Torque Per Ampere |
| PM | Permanent Magnet |
| PMSM | Permanent Magnet Synchronous Motor |
| $\mathbf{U}^{e}_{dq,s}$ | Voltage of Stator |
| $\mathbf{U}^{e}_{dq,r}$ | Voltage of Inner Rotor |
| $\mathbf{i}^{e}_{dq,s}$ | Current of Stator |
| $\mathbf{i}^{e}_{dq,r}$ | Current of Inner Rotor |
| $\mathbf{r}_{s}$ | Resistance of Stator |
| $\mathbf{r}_{r}$ | Resistance of Inner Rotor |
| $\boldsymbol{\psi}^{e}_{dq,s}$ | Flux of Stator |
| $\boldsymbol{\psi}^{e}_{dq,r}$ | Flux of Inner Rotor |
| $\omega$ | Angular Speed of Outer Rotor |
| $\omega_{r}$ | Angular Speed of Inner Rotor |
| $\psi_{m1}$ | Stator Winding Flux of Permanent Magnet |
| $\psi_{m2}$ | Inner Rotor Winding Flux of Permanent Magnet |
| $L_{sd}$ | d-axis Inductance of Stator |
| $L_{sq}$ | q-axis Inductance of Stator |
| $L_{md}$ | d-axis Mutual Inductance |
| $L_{mq}$ | q-axis Mutual Inductance |
| $L_{rd}$ | d-axis Inductance of Inner Rotor |
| $L_{rq}$ | q-axis Inductance of Inner Rotor |
| $T_{out}$ | Electromagnetic Torque of Outer Rotor |
| $T_{in}$ | Electromagnetic Torque of Inner Rotor |
| $p$ | Number of Pole Pairs |
| $i_{qs}$ | q-axis Current of Stator |

Received: 21 Aug. 2017
Revised: 20 Oct. 2017 and 19 Nov. 2017
Accepted: 06 Dec. 2017
∗Corresponding author:
E-mail: hadi.afsharirad@gmail.com (H. Afsharirad)
Digital object identifier: 10.22098/joape.2006.3955.1312

| | |
|---|---|
| $i_{qr}$ | q-axis Current of Inner Rotor |
| $i_{ds}$ | d-axis Current of Stator |
| $i_{dr}$ | d-axis Current of Inner Rotor |
| $I_{\max}$ | Maximum Current of Stator and Inner Rotor |
| $\lambda_s$ | Lagrange Coefficient of Stator Current Constraint |
| $\lambda_r$ | Lagrange Coefficient of Rotor Current Constraint |
| $V_{ds}$ | d-axis Voltage of Stator |
| $V_{qs}$ | q-axis Voltage of Stator |
| $V_{\max}$ | Maximum Voltage of Stator and Inner Rotor |
| $V_{dr}$ | d-axis Voltage of Inner Rotor |
| $V_{qr}$ | q-axis Voltage of Inner Rotor |
| $J_r$ | Inertia of Inner Rotor |
| $J_{pm}$ | Inertia of Outer Rotor |

## 1. INTRODUCTION

With the decrease of global petroleum resources and the severity of worldwide air pollution, development for new technology of EV and HEV is becoming the focus in this field [1- 3].

In advanced HEVs, the gasoline internal combustion engine is required to work in only a very narrow speed region for the highest fuel efficiency regardless of the vehicle speeds. Under such a constraint, a CVT is needed for power split and combination in HEV applications. Two types of CVT have been developed, and the first is the so-called mechanical version of CVT as in [4]. An intelligent gear box, planetary gear set, has been used to interface the gasoline ICE and two electrical machines (one as a motor and another generator) in such a way that any desirable vehicle speeds are achievable while the ICE can be locked in the highest fuel efficiency narrow speed region. In this manner, the planetary gear set actually splits or combines the driving power from both the ICE and electric motors. The second type of CVT is proposed in the electrical version, without mechanical gears, the so-called electrical variable transmission [5], [6].

In recent years, researchers have paid more and more attention to the research of dual mechanical port electric machine because it can achieve an electric variable transmission and can be used in HEV. A dual-mechanical-port electric machine has been proposed and discussed for HEV applications. The DMPM, with a single and compact package, potentially achieves all the functions and benefits that existing full HEV technologies could be achieved. The planetary gear set will not be used in HEVs based on DMPM traction systems [7].

The DMPMs with different outer rotors have been proposed [8-10]. This paper is studying modeling and control of the PM DMPM. Base on the modeling and structure of PM DMPM, the control methods of PMSM can be applied to the DMPM.

The control techniques for conventional Permanent Magnet Synchronous Motor have been widely studied. Field oriented control has been one of the most popular control methods [11], [12]. It is necessary for HEV as well as many other applications, to operate over both a wide speed range and high efficiency. Therefore, a control strategy, which uses MTPA control at low speed and FW control at high speed, was demonstrated in [13-15].

In FOC of permanent magnet synchronous machines, for simplicity, it is common that direct axis current is controlled to be zero. Although application of this method has the advantage of torque control linearity, it leads to a decrease in machine torque capacity because of losing reluctance torque. MTPA strategy fully utilizes the reluctance torque and maximizes the torque capacity of the machine therefore dynamic response of the overall drive system is increased. Furthermore, the MTPA method can also achieve the objective of minimum copper loss [16].

FW control is widely implemented for PMSM in high speed applications. The principle of FW control in PMSMs is that the air-gap flux can only be weakened by applying a demagnetizing armature current component along the d-axis of the permanent magnets. Since the output torque is proportional to product of air-gap flux and q-axis current component, such torque can be reduced with FW control [13-15].

In [2], [17-18], vector control of DMPM was proposed, but MTPA and FW algorithms are needed to fully utilize the potential of DMPM.

In this paper, FOC of dual mechanical port machine using maximum torque per ampere and Flux weakening is proposed. The organization of remaining paper as follows. In Section 2, the physical and mathematical model of DMPM will be discussed. Then, control algorithm, MTPA strategy, FW control and decoupling and feedforward algorithm for current controller are

described in Section 3. Obtained results are presented in section 4 and finally, conclusions are presented in the last section.

## 2. DMPM MODEL

### 2.1. Physical Model

DMPM consists of one stator and two rotors as shown in Fig. 1. The inner rotor is wounded but the outer rotor is permanent magnet rotor. The inner rotor is rigidly connected with engine crankshaft and the outer rotor is connected with drive shaft. A clutch is designed between the inner and outer rotors.

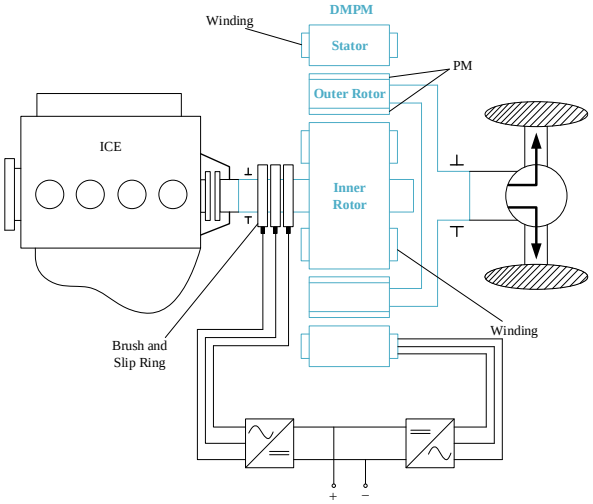


**Fig. 1.** Dual mechanical port machine use in HEV

### 2.2. Mathematical Model

In this section, the mathematical model of DMPM in synchronous reference frame is constructed as an integrated motor, which utilizes magnetic coupling between to air gaps is presented [18]. Voltage and flux equation of stator and inner rotor in synchronous reference frame are:

$$\left[\mathbf{U}^{e}_{dq,s}\right] = \mathbf{r}_s\left[\mathbf{i}^{e}_{dq,s}\right] + \frac{d\left[\boldsymbol{\psi}^{e}_{dq,s}\right]}{dt} - \omega\begin{bmatrix}0 & 1\\ -1 & 0\end{bmatrix}\left[\boldsymbol{\psi}^{e}_{dq,s}\right] \quad (1)$$

$$\left[\boldsymbol{\psi}^{e}_{dq,s}\right] = \sqrt{\frac{3}{2}}\psi_{m1}\begin{bmatrix}1\\0\end{bmatrix} + \frac{3}{2}\begin{bmatrix}L_{sd} & 0\\ 0 & L_{sq}\end{bmatrix}\left[\mathbf{i}^{e}_{dq,s}\right] + \frac{3}{2}\begin{bmatrix}L_{md} & 0\\ 0 & L_{mq}\end{bmatrix}\left[\mathbf{i}^{e}_{dq,r}\right] \quad (2)$$

$$\left[\mathbf{U}^{e}_{dq,r}\right] = \mathbf{r}_r\left[\mathbf{i}^{e}_{dq,r}\right] + \frac{d\left[\boldsymbol{\psi}^{e}_{dq,r}\right]}{dt} - (\omega-\omega_r)\begin{bmatrix}0 & 1\\ -1 & 0\end{bmatrix}\left[\boldsymbol{\psi}^{e}_{dq,r}\right] \quad (3)$$

$$\left[\psi^{e}_{dq,r}\right] = \sqrt{\frac{3}{2}}\psi_{m2}\begin{bmatrix}1\\0\end{bmatrix} + \frac{3}{2}\begin{bmatrix}L_{rd} & 0\\ 0 & L_{rq}\end{bmatrix}\left[i^{e}_{dq,r}\right] + \frac{3}{2}\begin{bmatrix}L_{md} & 0\\ 0 & L_{mq}\end{bmatrix}\left[i^{e}_{dq,s}\right] \quad (4)$$

The electromagnetic torque of the rotor in DMPM can be expressed as:

$$T_{out} = p[\sqrt{\frac{3}{2}}(i_{qs}\psi_{m1} + i_{qr}\psi_{m2}) + \frac{3}{2}(L_{sd} - L_{sq})i_{ds}i_{qs} + \frac{3}{2}(L_{rd} - L_{rq})i_{dr}i_{qr} + \frac{3}{2}(L_{md} - L_{mq})(i_{ds}i_{qr} + i_{qs}i_{dr})] \quad (5)$$

$$T_{in} = -p[(\sqrt{\frac{3}{2}}\psi_{m2}i_{qr} + \frac{3}{2}L_{md}i_{ds}i_{qr} - \frac{3}{2}L_{mq}i_{qs}i_{dr}) - \frac{3}{2}(L_{rq} - L_{rd})i_{dr}i_{qr}] \quad (6)$$

## 3. CONTROL STRATEGY

FOC is a popular control method for AC machine. The FOC block diagram of dual mechanical port machine has been shown in Fig. 2. The DMPM controller consists of two independent speed loops, one for outer PM rotor and another for inner wound rotor. In each speed loop, there are two current loops, one for current regulation in the q-axis and another in the d-axis. In general, the speed controller is a regular PI controller. While the current controller usually has to be designed with a feed forward compensation. For traction applications, the MTPA control is the most effective strategy in the low speed regions while the FW control is necessary in high speed applications. Although MTPA and FW employ different algorithms, they are FOC methods in their nature.

### 3.1. MTPA Control Algorithm

In hybrid electrical vehicle applications, the dynamic response of inner rotor is not very important, because this rotor is connected to ICE and is used in certain points where the ICE have high efficiency and low pollution. So in MTPA method the torque of outer rotor which is connected to vehicle wheels is going to be analyzed.

In conventional control of DMPM if $i_{ds}$ and $i_{dr}$ are considered zero, the outer rotor torque is proportional to $i_{qs}$ and $i_{qr}$. In this case, reluctance torque is ignored. MTPA method increases drive efficiency. By selecting the appropriate value for d-axis currents in this method, the maximum torque of outer rotor is combination of electromagnetic torque and reluctance torque.

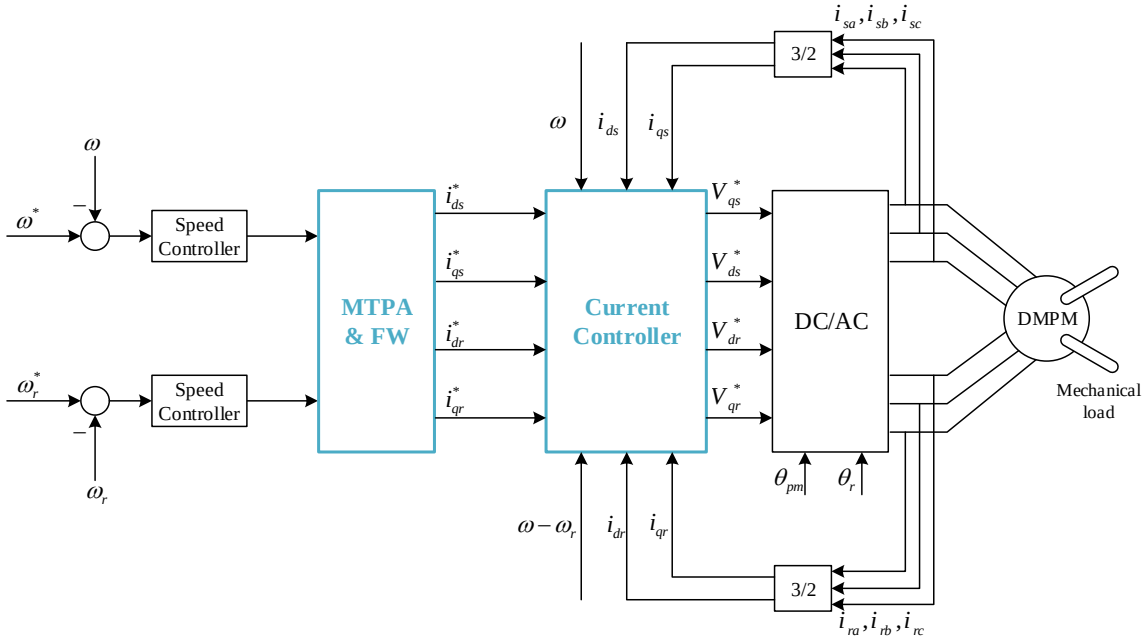


**Fig. 2.** Block diagram of DMPM controller

Stator and rotor currents constraints are expressed by Eqs. (7) and (8).

$$i_{qs}^2 + i_{ds}^2 \le I_{\max}^2 \tag{7}$$

$$i_{qr}^2 + i_{dr}^2 \le I_{\max}^2 \tag{8}$$

To have maximum torque, these constraints have been applied to outer rotor torque equation and derivative of obtained equations toward d-axis and q-axis currents is equal to zero.

$$\frac{\partial}{\partial i_{qs}}\left(T_{out} + \lambda_s(I_{\max}^2 - i_{qs}^2 - i_{ds}^2) + \lambda_r(I_{\max}^2 - i_{qr}^2 - i_{dr}^2)\right) = 0 \tag{9}$$

$$\frac{\partial}{\partial i_{ds}}\left(T_{out} + \lambda_s(I_{\max}^2 - i_{qs}^2 - i_{ds}^2) + \lambda_r(I_{\max}^2 - i_{qr}^2 - i_{dr}^2)\right) = 0 \tag{10}$$

$$\frac{\partial}{\partial i_{qr}}\left(T_{out} + \lambda_s(I_{\max}^2 - i_{qs}^2 - i_{ds}^2) + \lambda_r(I_{\max}^2 - i_{qr}^2 - i_{dr}^2)\right) = 0 \tag{11}$$

$$\frac{\partial}{\partial i_{dr}}\left(T_{out} + \lambda_s(I_{\max}^2 - i_{qs}^2 - i_{ds}^2) + \lambda_r(I_{\max}^2 - i_{qr}^2 - i_{dr}^2)\right) = 0 \tag{12}$$

By analyze Eqs. (9) to (12) and eliminate Lagrange coefficients and simplify them, Eqs. (13) and (14) will be obtained.

$$\sqrt{\frac{2}{3}}\varphi_{m1} i_{ds} + (L_{sd} - L_{sq})(i_{ds}^2 - i_{qs}^2) + (L_{md} - L_{mq})(i_{dr} i_{ds} - i_{qr} i_{qs}) = 0 \tag{13}$$

$$\sqrt{\frac{2}{3}}\varphi_{m2} i_{dr} + (L_{rd} - L_{rq})(i_{dr}^2 - i_{qr}^2) + (L_{md} - L_{mq})(i_{ds} i_{dr} - i_{qs} i_{qr}) = 0 \tag{14}$$

By substituting Eqs. (15) and (16) in Eqs. (13) and (14), a nonlinear system of two equations with two variables will be obtained.

$$i_{qs} = sign(I_s)\sqrt{I_s^2 - I_{ds}^2} \tag{15}$$

$$i_{qr} = sign(I_r)\sqrt{I_r^2 - I_{dr}^2} \tag{16}$$

These equations cannot be solved by analytical method. So these two equations are solved in MATLAB for different stator and rotor currents by 0.1 step size and are placed in Lookup Table.

### 3.2. FW Control Algorithm

For traction applications, drive systems require a wide constant power speed range. Since back-EMF is proportional to rotor speed and air gap flux, high speeds leads to a higher back-EMF value than maximum output voltage of drive system. So, when back-EMF reaches the maximum voltage value, motor torque decreases rapidly.

Therefore, air gap flux should be reduced to increase speed. Because the magnetic field is produced by PMs, flux weakening is not possible in this way, so flux weakening is produced by generation a proper negative d-axis current. In FW strategy two current constraints according to Eqs. (7) and (8) and two voltage constraints according to Eqs. (17) and (18) for DMPM are considered.

$$V_{qs}^2 + V_{ds}^2 \le V_{\max}^2 \tag{17}$$

$$V_{qr}^2 + V_{dr}^2 \le V_{\max}^2 \tag{18}$$

By substituting Eqs. (1) to (4) in Eqs. (17) and (18), voltage constraint equations are obtained.

$$\frac{V_{\max}^2}{\omega^2} = \frac{9}{4}\left(\left(L_{sq} i_{qs} + L_{mq} i_{qr}\right)^2 + \left(\sqrt{\frac{2}{3}}\varphi_{m1} + L_{sd} i_{ds} + L_{md} i_{dr}\right)^2\right) \tag{19}$$

$$\frac{V_{\max}^2}{\left(\omega - \omega_r\right)^2} = \frac{9}{4}\left(\left(L_{rq} i_{qr} + L_{mq} i_{qs}\right)^2 + \left(\sqrt{\frac{2}{3}}\varphi_{m2} + L_{rd} i_{dr} + L_{md} i_{ds}\right)^2\right) \tag{20}$$

Obtained currents of MTPA control method, $V_{\max} = 500\ \text{V}$ and $I_{\max} = 30A$ are applied in Eqs. (19) and (20). Base speeds are calculated according to Table 1:

**Table 1.** Calculated base speed

| $I_s$ $(A)$ | $I_r$ $(A)$ | $\omega$ $(rad/s)$ | $\omega - \omega_r$ $(rad/s)$ | $n$ $(rpm)$ | $n - n_r$ $(rpm)$ |
|---|---|---|---|---|---|
| 30 | 30 | 796.66 | 1849.9 | 1901.86 | 4416.31 |
| 30 | 0 | 862.95 | 2753.45 | 2060.14 | 6574.45 |

For HEV application inner rotor is inert or rotates with a certain speed (ICE speed) usually between 2000 to 3000 rpm. Also in DMPM where inner rotor current is unequal to zero, stator current is unequal to zero. Therefor FW control operational modes are as bellow:

1. No current passes in the inner rotor winding ($I_r = 0$).

This mode is occurred when outer rotor speed is more than 2060.14 rpm. In this mode the negative value of $I_{ds}$ will be increased and also inner rotor will be working in certain points. Therefor inner rotor voltage constraints are always established.

If $I_r = 0$, Eq. (19) is simplified as following equation:

$$\frac{V_{\max}^2}{\omega^2} = \frac{9}{4}\left(L_{sq}^2 i_{qs}^2 + \left(\sqrt{\frac{2}{3}}\varphi_{m1} + L_{sd} i_{ds}\right)^2\right) \tag{21}$$

With using stator current constraint Eq. (22) will be obtained:

$$i_{qs} = \sqrt{I_{\max}^2 - i_{ds}^2} \tag{22}$$

If Eq. (22) is substituted in Eq. (21) and simplifying, a quadratic equation in terms of $i_{ds}$ will be obtained.

$$\left(L_{sd}^2 - L_{sq}^2\right) i_{ds}^2 + 2\sqrt{\frac{2}{3}}\varphi_{m1} L_{sd} i_{ds} + \frac{2}{3}\varphi_{m1}^2 + L_{sq}^2 I_{\max}^2 - \frac{V_{\max}^2}{\frac{9}{4}\omega^2} = 0 \tag{23}$$

With solving Eq. (23) two answers for $i_{ds}$ will be found. It should be noted that $i_{ds}$ must be negative.

So the acceptable answer will be as follows:

$$i_{ds} = \frac{-\sqrt{\frac{2}{3}}\varphi_{m1} L_{sq} + \sqrt{\left(\sqrt{\frac{2}{3}}\varphi_{m1} L_{sd}\right)^2 - \left(L_{sd}^2 - L_{sq}^2\right)\left(\frac{2}{3}\varphi_{m1}^2 + L_{sq}^2 I_{\max}^2 - \left(\frac{V_{\max}}{\frac{3}{2}\omega}\right)^2\right)}}{\left(L_{sd}^2 - L_{sq}^2\right)} \tag{24}$$

2. Currents of both windings are unequal to zero.

This mode is occurred when outer rotor speed is more than 1901.86 rpm. In this mode by considering negative value for $i_{ds}$ in inner rotor voltage constraints equations and working in certain points, the inner rotor voltage constraints are always established.

If Eq. (22) is substituted in Eq. (19) and simplifying the equation a nonlinear equation in terms of $i_{ds}$ will be obtained.

$$\left(L_{sd}^2 - L_{sq}^2\right) i_{ds}^2 + 2L_{sd}\left(\sqrt{\frac{2}{3}}\varphi_{m1} + L_{md} i_{dr}\right) i_{ds} + 2L_{sq} L_{mq}\sqrt{I_{\max}^2 - i_{ds}^2} + L_{sq}^2 I_s^2 + L_{mq}^2 i_{qr}^2 + \frac{2}{3}\varphi_{m1}^2 + L_{md}^2 i_{dr}^2 + 2\sqrt{\frac{2}{3}}\varphi_{m1} L_{md} i_{dr} - \frac{V_{\max}^2}{\frac{9}{4}\omega^2} = 0 \tag{25}$$

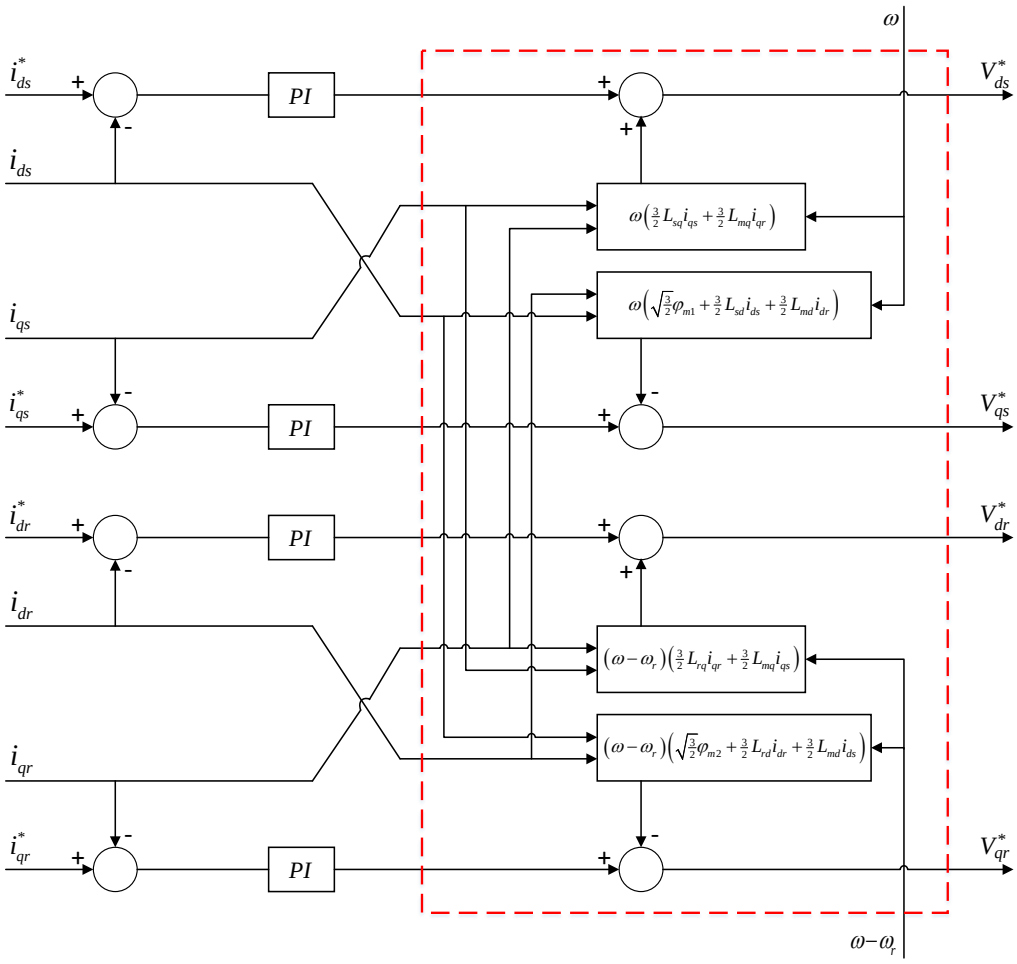


**Fig. 3.** Decoupling and feedforward algorithm scheme in current controller

Nonlinear equation Eq. (25) is insolvable in analytical method. This equation is solved in different outer rotor speeds and inner rotor currents respectively with 5 rpm and 0.1 A steps in MATLAB and are placed in Lookup Table.

### 3.3. Current controllers

In FOC, the current controller has a crucial role. Generally, the current controller has to be designed with a decoupling and feedforward algorithm. The reason stems from the fact that in the synchronous frame, the DMPM model presents coupling terms between d and q axes and inner rotor and stator. These terms can be considered as disturbances that complicate the design of PI controllers and reduce the overall dynamic performances. A decoupling and feedforward algorithm has been implemented in the drive, as shown in Fig. 3. This algorithm reduces the cross-coupling effects between the two axes and two windings and simplifies the PI controller design.

## 4. SIMULATION AND RESULTS

The proposed control of DMPM has been simulated in MATLAB/simulink. The DMPM specification is shown in Table 2.

**Table 2.** DMPM parameters

| | | | |
|---|---|---|---|
| $P$ | 4 | $L_{mq}(mH)$ | 1.5 |
| $R_s(\Omega)$ | 0.035 | $L_{md}(mH)$ | 0.5 |
| $R_r(\Omega)$ | 0.02 | $\psi_{m1}(wb)$ | 0.2 |
| $L_{sq}(mH)$ | 15 | $\psi_{m2}(wb)$ | 0.15 |
| $L_{sd}(mH)$ | 9 | $J_r(kg/m^2)$ | 0.025 |
| $L_{rq}(mH)$ | 4.5 | $J_{pm}(kg/m^2)$ | 0.08 |
| $L_{rd}(mH)$ | 3 | | |

This simulation has three parts. The first part shows difference of FOC control with and without MTPA and expresses MTPA advantages. The second part evaluate the performance of this drive system in high speeds with

the FW control. The last part simulates a simplified driving cycle of HEV. The driving cycle contains the HEV from starting to stop with several driving actions taken in between.

### 4.1. MTPA Control

This part of simulation is divided into three intervals. Speeds and torques of two rotors in these intervals are shown in Fig. 4.

In the first interval outer rotor is accelerated from 0 to 1500 rpm. When MTPA control is used in this interval, outer rotor torque is increased 34.38% and rise time of outer rotor speed is decreased 0.22 s. The steady state error of outer rotor speed is 0.17%.

The second interval starts in 3 second. At this interval, outer rotor already at 1500 rpm and inner rotor is accelerated from 0 to 1000 rpm. By applying MTPA control, Inner rotor torque is increased 9.5% and rise time of inner rotor speed is decreased 0.02 s. The steady state error of inner rotor speed is 0.01%.

In the last interval the outer rotor speed reduces from 1500 rpm to -1000 rpm. In this interval like first interval with 34.38% increasing of torque in inverse direct, the time of these changes is reduced 0.36 s. The steady state error of outer rotor speed is 0.44%.

### 4.2. FW Control

In this part, outer rotor speed is higher than base speeds, so it is necessary to use FW control. Simulation results of DMPM in high speed are shown in Fig. 5. At the beginning of this part the outer rotor is accelerated from 0 to 4000 rpm and the inner rotor is standstill. Drive system implements the MTPA control until 2060.14 rpm. Then, it employs the FW control, when the speed is above 2060.14 rpm. At this period inner rotor current is equal zero, therefore the FW control mode is 1. At 7 s outer rotor speed reduces from 4000 rpm to -2500 rpm. During these changes, ICE delivers a mechanical torque to inner rotor. So the FW control mode is 2. Inner rotor phase A voltage curve shows inner rotor voltage constraints are established during this part.

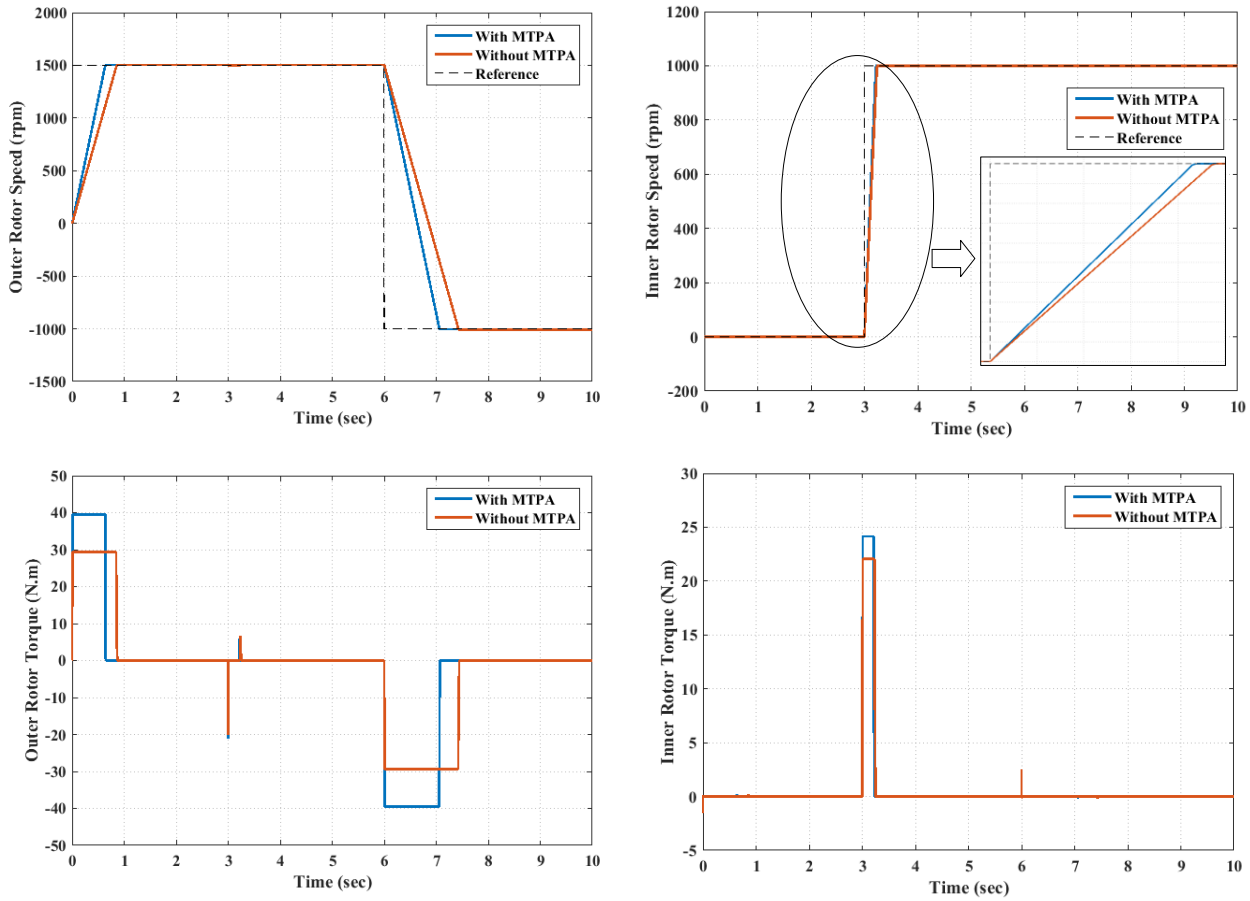


**Fig. 4.** Simulation result with and without MTPA

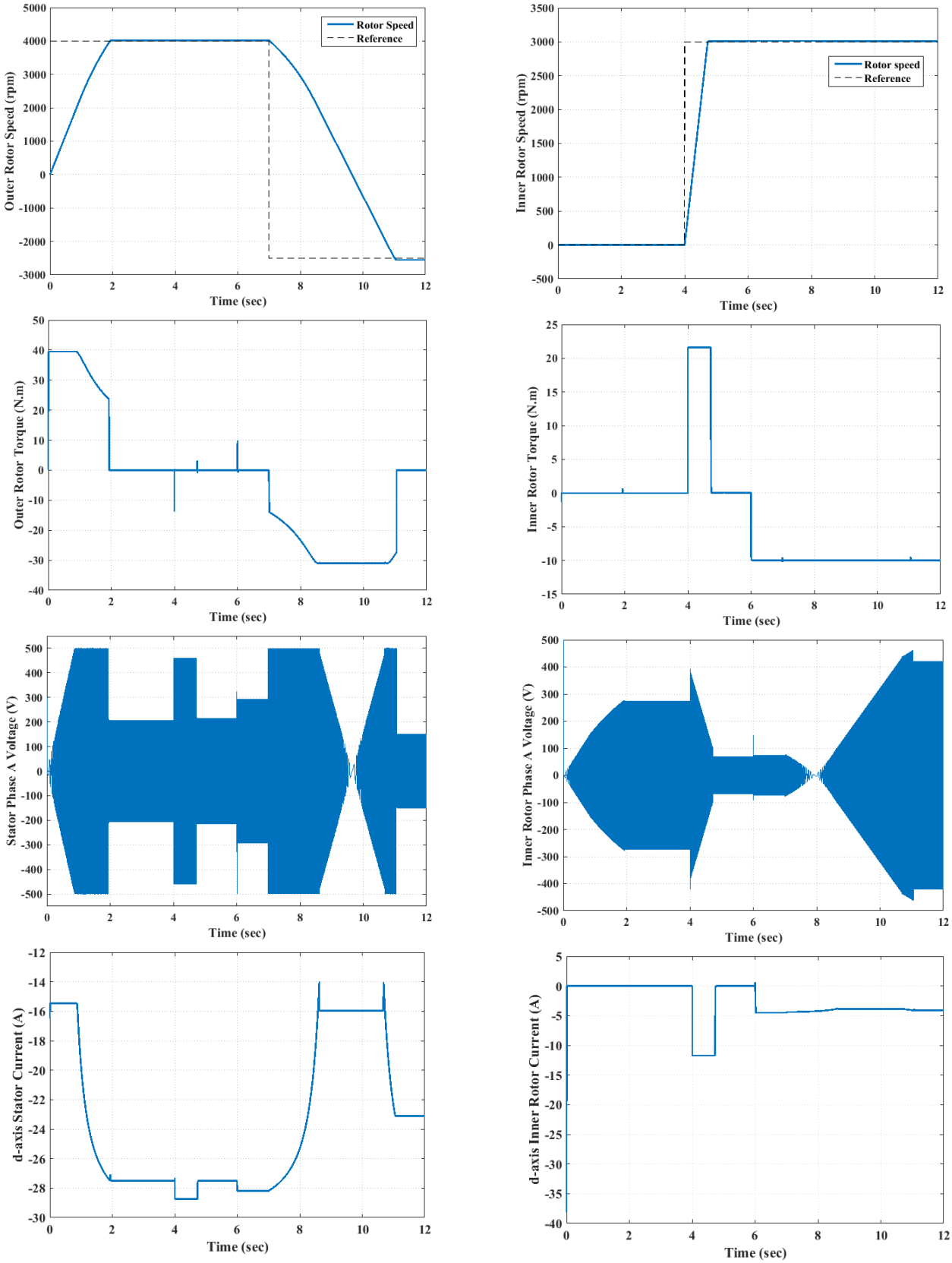


**Fig. 5.** Simulation results in high speed

### 4.3. Simplified Driving Cycle of HEV

The operations of DMPM are simulated in 6 intervals. The results are shown in Fig. 6.

1) The outer rotor speed is increased from 0 to 3000 rpm. Inner rotor is not excited and is stanstill. During this interval, electromagnetic torque is generated by the stator currents and the DMPM is in pure electrical mode.

2) In the second interval, the inner rotor speed is increased from 0 to 3500 rpm without firing on the ICE. Before inner rotor speed reaches to 3000 rpm (synchronous speed), this rotor recieves more power than it needs from outer rotor. The extra power is stored in electric source by the winding of inner rotor.

3) The ICE provides 10 N.m mechanical torque to the inner rotor. This interval covers the period from 5 s to 11 s. In this period stator and outer rotor are sending power to battery.

4) This interval starts at 7 s. As shown, outer rotor is accelerated from 3000 to 3300 rpm and is reduced to 3000 rpm again.

5) In the last interval, the outer rotor speed is decreased to 0 rpm and electrical energy is recoverd and DMPM functions as a generator.

## 5. CONCLUSIONS

In this paper, use of FOC for DMPM in HEV as an EVT is proposed. Some advantages of DMPM are that two ports of the DMPM work in motor and generator modes at the same time and the planetary gear set will not be used in the HEVs propelled by the DMPM. This machine with only a compact package potentially achieves all functions and benefits that the traditional full HEV technologies can be achieved.

The FOC for DMPM proposed and simulated. The percent of steady state errors in inner and outer rotors are less than 1%. By applying MTPA the dynamic response of system improves considerably. Flux weakening control can further extend the speed range of DMPM. Using decoupling and feedforward algorithm current controller design is simple and reduces disturbances of q and d axis currents more. The simulation results verify DMPM superiority in full HEV application.

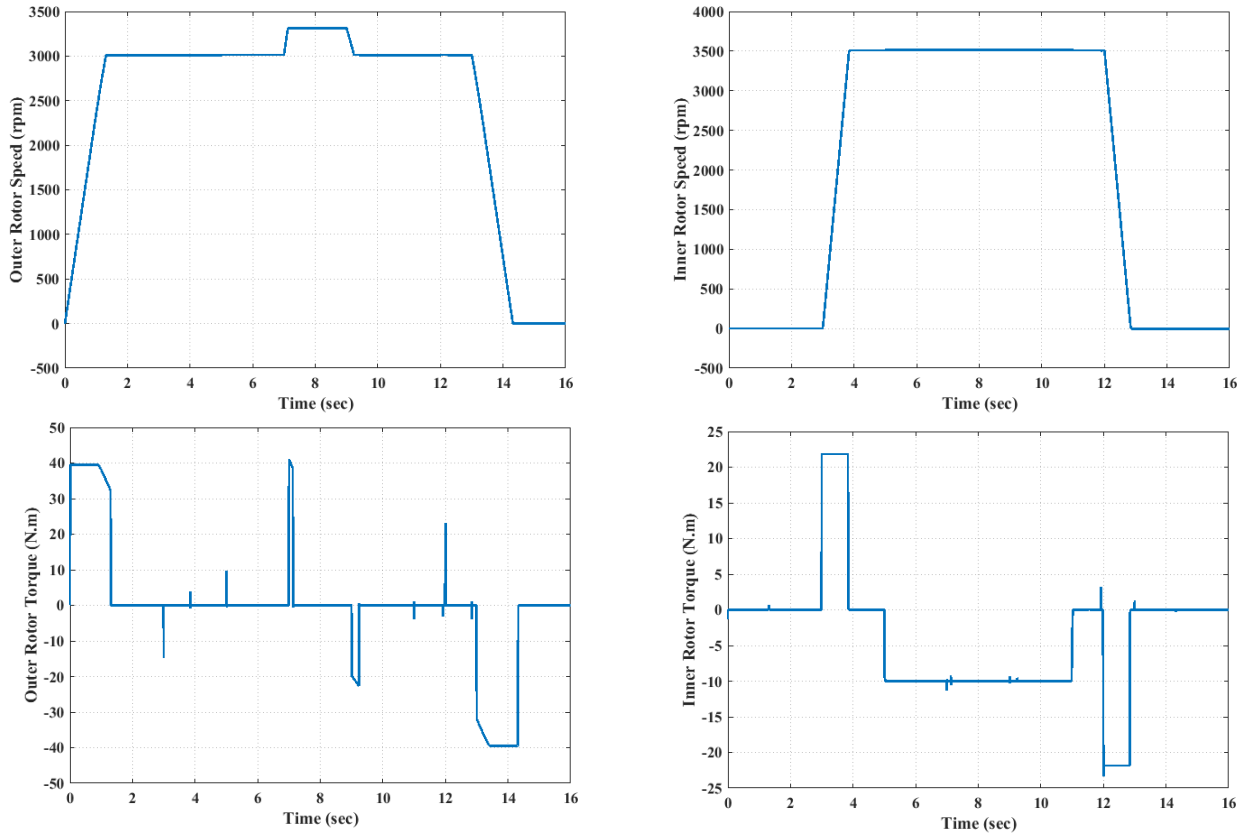


**Fig. 6.** Simulation results of simplified driving cycle HEV

## REFERENCES


[1] L. Li, Q. Zhao, G. Shi and H. Wang, "Analysis of feasibility of double-rotor motor applied to hybrid electric vehicle," *IEEE Veh. Power Propul. Conf.*, Harbin, China, September 3-5, 2008.

[2] M. Moazen and M. Sabahi, "Electric differential for an electric vehicle with four independent driven motors and four wheels steering ability using improved fictitious master synchronization strategy," *J. Oper. Autom. Power Eng.*, vol. 2, no. 2, pp. 141-150, 2014.

[3] N. Bagheri and H. Alipour, "Yaw rate control and actuator fault detection and isolation for a four-wheel independent drive electric vehicle," *J. Oper. Autom. Power Eng.*, vol. 5, no. 1, pp. 83-95, 2017.

[4] L. Xu, Y. Zhang and X. Wen, "Multioperational modes and control strategies of dual-mechanical-port machine for hybrid electrical vehicles," *IEEE Trans. Ind. Appl.*, vol. 45, no. 2, 2009.

[5] E. Nordlund, P. Thelin and C. Sadarangani, "Four-quadrant energy transducer for hybrid electric vehicles," Proc. of the *15th Int. Congr. Electron Microsc.*, pp. 37-44, Brugge, Belgium, August 25-28, 2002.

[6] M. J. Hoeijmakers and J. A. Ferreira, "The electric variable transmission," *IEEE Trans. Ind. Appl.*, vol. 42, no. 4, pp. 1092-1100, 2006.

[7] A. Ghayebloo and A. Radan, "Superiority of dual-mechanical-port-machine-based structure for series-parallel hybrid electric vehicle applications," *IEEE Trans. Veh. Technol.*, vol. 65, no. 2, 2016.

[8] L. Xu, "Dual-mechanical-port electric machines-concept and application of a new electric machine to hybrid electrical vehicles," *IEEE Ind. Appl. Mag.*, vol. 15, no. 4, pp. 44-51, 2009.

[9] S. Cui, Y. Yuan and T. Wang, "Research on switched reluctance double rotor motor used for hybrid electric vehicle," Proc. of the *Int. Conf. Elect. Mach. Syst.*, pp. 3393-3396, 2008.

[10] H. Cai and L. Xu, "Modeling and control for cage rotor dual mechanical port electric machine-part I: model development," *IEEE Trans. Energy Convers.*, vol. 30, no. 3, pp. 957-965, 2015.

[11] G. Chandaka and G. Prasanth, "Direct torque control and field oriented control of PMSM using SVPWM technique," *Int. J. Adv. Res. Sci. Eng.*, vol. 3 no. 11, 2014.

[12] A. Khlaief, M. Abassi, M. Boussak and M. Gossa, "DSP based SVPWM technique for field oriented speed control of permanent magnet synchronous motor drive," Proce of the *Int. Conf. Sci. Tech. Autom. Control*, 2009.

[13] V. R. Jevremovic and D. P. Marcetic, "Closed-loop flux-weakening for permanent magnet synchronous motors," Proc. of the *4th IET Conf. Power Electron. Machines Drives*, pp. 717-721, 2008.

[14] J. M. Kim and S. K. Sul, "Speed control of interior permanent magnet synchronous motor drive for the flux weakening operation," *IEEE Trans. Ind. Appl.*, vol. 33, no. 1, pp. 43-48, 1997.

[15] S. Morimoto, M. Sanada and Y. Takeda, "Wide-speed operation of interior permanent magnet synchronous motors with high-performance current regulator," *IEEE Trans. Ind. Appl.*, vol. 30, no. 4, pp. 920-926, 1994.

[16] C. T. Pan and S. M. Sue, "A linear maximum torque per ampere control for IPMSM drives over full-speed range," *IEEE Trans. Energy Convers.*, vol. 20, no. 2, 2005.